Available online at www.sciencedirect.com

ScienceDirect

journal homepage: www.elsevier.com/locate/he

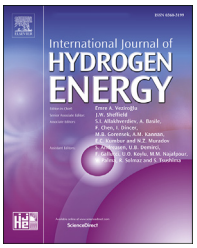

Injection of gaseous hydrogen into a natural gas pipeline

I. Eames, M. Austin, A. Wojcik

Centre for Engineering in Extreme Environments, University College London, Gower Street, London WC1E 7JE, UK

HIGHLIGHTS

- Injection of hydrogen through a T junction leads to poor mixing and high concentrations of hydrogen on pipe walls.
- Stratification leads to higher hydrogen concentration near upper pipe wall.
- Higher hydrogen concentration on walls leads to the embrittlement of high-tensile steels.
- ASME B31.3 indicates that gas pressure needs to be decreased which contrasts with the energy flux constraint.

ARTICLE INFO

Article history:
Received 9 February 2022
Received in revised form
28 May 2022
Accepted 31 May 2022
Available online xxx

Keywords:
Injection
Mixing
Embrittlement
Blending

ABSTRACT

The injection of pure hydrogen at a T-junction into a horizontal pipe carrying natural gas is analysed computationally to understand the influence of blending and pipe geometry (diameter ratio, various 90° orientations) on mixing, for a target of 4.8–20% volume fraction hydrogen blend. The strongly inhomogeneous distribution of hydrogen within the pipe flow and on the pipe walls could indicate the location of potential pipe material degradation including embrittlement effects.

The low molecular mass of hydrogen reduces the penetration of a side-branch flow and increases the buoyancy forces leading to stratification with high hydrogen concentrations on the upper pipe surface, downstream of the branch. Top-side injection leads to the hydrogen concentration remaining >40% for up to 8 pipe diameters from the injection point for volumetric dilutions ($\mathcal{D}$) less than 30%. Under-side injection promotes mixing within the flow interior and reduces wall concentration at the lower surface, compared to top-side injection.

The practical implications for these results, in terms of mixing requirements and the contrasting constraint of codes of practice and energy demands, are discussed.

Introduction

The international drive to limit climate change is centered around reducing the emission of CO_2 into the atmosphere. The largest domestic component of CO_2 emission in the UK – 3000 kg per household per annum – comes simply from heating. The current proposal is to reduce CO_2 generation through the increased reliance on heat pumps or by switching to natural gas blended with increasing proportions of hydrogen. The general proposition is that blending hydrogen at concentrations 5–20% by volume with natural gas, would

E-mail addresses: i.eames@ucl.ac.uk (I. Eames), m.austin@ucl.ac.uk (M. Austin), a.wojcik@ucl.ac.uk (A. Wojcik).
https://doi.org/10.1016/j.ijhydene.2022.05.300

not require changes in the end of use devices (such as boilers), with a long term expectation that the hydrogen fraction could be raised and varied within different piping networks. Most attention is focused on the production of green hydrogen from renewable energy sources, such as wind or solar, that will enable excess energy to be converted to hydrogen [1–3]. From a network perspective, a key question is where the hydrogen could be injected into the gas network since the source of hydrogen production is unlikely to be coincident with the inlet of the pipe network. This has been the topic of considerable discussion where research has looked at the steady state and transient distribution of hydrogen in a natural gas pipeline and its influence on pressure drops and resistance [2,4,5].

The key element of hydrogen injection is how it is introduced into the network. In this paper we look at issues associated with creating a blended mixture through the injection of pure hydrogen into natural gas in a pipe flow via a simple 90° branch and the implications for material selections. In the nineteenth century, hydrogen was a component of 'town' gas supplies for some considerable time due to the method of production (from coal), with hydrogen concentrations up to 30% by volume (see Ref. [6]), along with a number of corrosive sulphurous by-products. Some locations, such as Honolulu, still retain the use of town gas. Hydrogen is commonly transported in liquid or gas form over considerable distances (at pressure) in infrastructure designed *a priori* to accommodate hydrogen. From a metallurgical perspective, hydrogen has the potential to permeate into many materials including the steels commonly used in gas pipelines. The UK engineering challenge is to repurpose a network, where the allowable maximum concentration of hydrogen is 0.1%, into a network capable to supporting far greater hydrogen levels. Currently the UK gas transmission network is predominately fabricated in steel while the local distribution network includes a significant proportion of composites and polymers [7]. The limit of hydrogen volume fraction is based on local laws, which vary significantly across Europe, from 0.5% in Sweden, 4% in Austria and Switzerland, 6% in France to 12% in the Netherlands [8]. The upper limit on hydrogen concentration depends on the materials selected and over-pressure constraints exercised through local codes of practice. It is clear that these upper limits must be safely raised to deliver green hydrogen.

Blending hydrogen into natural gas introduces two diametrically opposite constraints from energy delivery and material selection. The first consequence is that while the (useable) energy density of pure hydrogen is greater than natural gas (at 145 MJ kg^{-1} compared to 53 MJ kg^{-1}), hydrogen has a density which is 9 times lower, meaning that at fixed pressure, blending hydrogen reduces the effective energy (per *unit volume*). This can only be remediated by higher blend flow rates or raised pressure. The macroscopic consequences of hydrogen blends on pumping configuration have been discussed in Ref. [9]. The second consequence is that hydrogen embrittles carbon steel, particularly high tensile steels, and this may require a reduction in pressure (as per [10]) as a means of reducing the likelihood of failure.

Gases streams (with compositional or temperature differences) are usually blended by injecting one gas through a side branch or *T*-junction into a main gas header pipe [11]. A typical scenario is top-side injection into a horizontal pipe flow (see Fig. 1). The low density of hydrogen introduces two fluid mechanical problems - it has a low penetration factor owing to low inertia and buoyancy effects may be significant with mixing greatly reduced and the mixture tending to stratify [12]. While there has been considerable research into the combustion of injected hydrogen jets [13] or injected into pipes via microchannels [14], there has been little research on injecting hydrogen into natural gas pipes in scenarios when buoyancy effects are important.

At the core of the blending issue is the mixing that occurs due to hydrogen injection under conditions typical within industry. Blending typically occurs at a *T*-junction – as shown in Fig. 1 where pure hydrogen is injected into a horizontal flow of natural gas (to be modelled here as methane). The two key variables are the mixing ratio or dilution factor of the configuration and the *T*-junction geometry. Two variants of the standard *T*-junction are the centrally placed top-side and under-side branch junction and the laterally displaced – or Hillside – junction which is set to generate swirl in the header pipe. Whilst it is traditional to inject from above, it is worth contrasting with underside injection where the buoyant rise of hydrogen has a greater potential to promote mixing. This is further discussed below.

Mixing at *T*-junctions is extremely well-studied, particularly when thermal effects are important. The majority of the published studies relate to the mixture of hot and cold water (under pressure) [15–18] with attention paid to the thermal fluctuations on walls which generate cyclic thermal loading and the potential for crack formation [17,19,20]. In this paper, the scientific gap comes from the unusually large density contrast from hydrogen injection which has no analogy to liquid systems. Of vital importance is to quantify the hydrogen concentration adjacent to the walls because this has a bearing on the potential for embrittlement. The assumption that mixing occurs almost immediately upon introduction is most definitely one that needs to be tested.

The influence of hydrogen on steels at moderate ambient temperatures is generally well-known [21]. Hydrogen uptake by a steel embrittles the metal via a number of atomistic mechanisms leading to increased fracture growth rates [22]. Embrittlement principally reduces the metal's ductility and in turn this affects mechanical properties such as fracture toughness. The toughness of a material is arguably of greater significance than its strength as it is the toughness that determines the practical strength of a material in the presence of the many types of defects, both intrinsic and introduced, that a material (and fabricated component) contains. A drop in toughness, accumulating over time, when combined with existing defects (for example, porosity or welding defects), can easily render design calculations ineffective.

Welds are also particularly susceptible to hydrogen embrittlement and its effects, this being a consequence of several factors including the presence of microstructured phases that are themselves already at lower toughness than the surrounding 'parent' material, but also the existence of defects (introduced during welding) and the likelihood of thermal residual stress (again due to the welding process), all of which combine to make welds by definition critical areas for cracking and failure. Embrittlement can also reduce component lifetimes when fatigue crack growth is considered.

Please cite this article as: Eames I et al., Injection of gaseous hydrogen into a natural gas pipeline, International Journal of Hydrogen Energy, https://doi.org/10.1016/j.ijhydene.2022.05.300

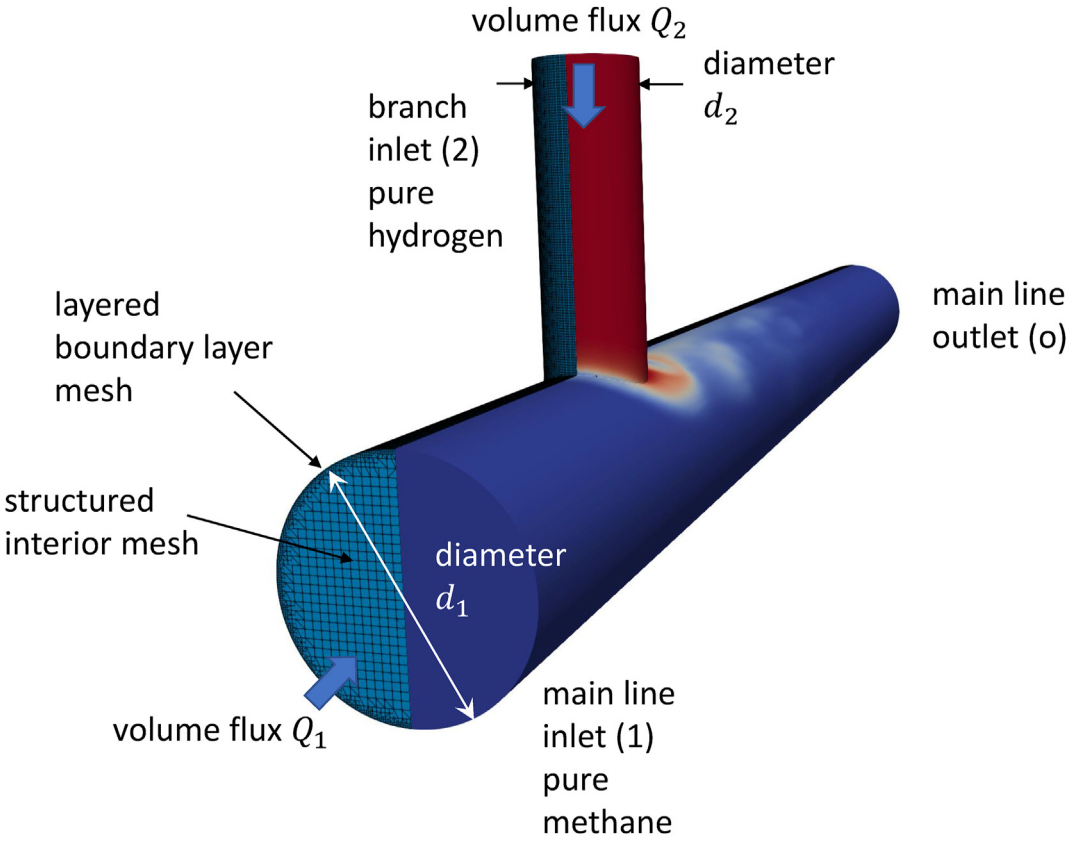

Fig. 1 – Schematic of a T-junction. The flow domain consists of a main inlet, branch inlet and outlet, which are labelled as 1, 2 and o respectively. The problem consists of the injection of pure hydrogen through the branch inlet into a main line through which pure methane is introduced. The notation used in the analysis and mesh quality are indicated.

This is, again, simply a consequence of the reduction in fracture toughness – making the critical crack size required for fracture much less, and hence reducing the time needed for such a crack to form under fatigue conditions. Hydrogen has also been found to accelerate fatigue crack growth rates per se, thus ensuring that the critical defect size is reached faster.

In this paper, a computational methodology is applied to explore the general influence of injection rates, geometry and direction on hydrogen mixing during injection. The typical range of values met in practice and modelling assumption are first elaborated before the details of the computational model are described. The distribution of hydrogen within the pipe are discussed in section on numerical results. The broad practical implications for hydrogen injection into pipes are discussed before conclusions are made.

Model description

In the UK, the current natural gas network consists of 18 inch (460 mm) diameter pipes operating at $p_1 = 6.9$ MPa ([23], see Table 6). The gas speed is typically about $u_1 = 10$ m s^{-1}. The gas temperature varies from 5° C to 45° C depending on proximity to the compressor station. The pipes are usually buried and the ground temperature (at 3 m below the surface) is relatively constant at around 11.2° C and is set here as $T_1 = 284$ K. The temperature of the injected hydrogen is taken to be $T_2 = 293$ K. While it is important to acknowledge and include thermal effects, the influence of temperature differences on density differences and buoyancy effects are negligible compared to compositional differences caused by hydrogen and methane. A schematic of the problem is shown in Fig. 1. As described earlier, this consists of a branch flow of pure hydrogen with a co-flow of natural gas. Natural gas is a complex mixture of gases [23] (see Table 3, p. 14) with the largest component being methane (92.42%), followed by nitrogen (3.67%) and ethane (3.02%). For simplicity, the main line flow is modelled as methane (with a molecular mass of $M_{CH_4} = 16$g mol^{-1}).

The requirement is to have a target *average* hydrogen volume concentration in the range of 5–20%. This is relevant because it has a bearing on the inlet condition. The local mass fraction of hydrogen is denoted as Y_{H_2} and since there are only two species present, the concentration of methane is $Y_{CH_4} = 1 - Y_{H_2}$. Under ideal gas conditions, the density of the main line inlet and branch inlet gas streams are determined by the local pressure and temperature through

$$\rho_1 = \frac{M_{CH_4} p_1}{R_g T_1}, \qquad \rho_2 = \frac{M_{H_2} p_2}{R_g T_2}, \tag{1}$$

Please cite this article as: Eames I et al., Injection of gaseous hydrogen into a natural gas pipeline, International Journal of Hydrogen Energy, https://doi.org/10.1016/j.ijhydene.2022.05.300

where R_g is the ideal gas constant and M is the molecular mass of the species. Given the (molar) concentration of hydrogen is $[H_2] = \frac{\overline{\rho} Y_{H_2}}{M_{H2}}$, where $\overline{\rho}$ is the local average mixture density, the (local) mole fraction of hydrogen is therefore

$$V_R = \frac{\beta}{1+\beta}, \tag{2}$$

where

$$\beta = \frac{Y_{H_2}}{1-Y_{H_2}} \frac{M_{CH_4}}{M_{H_2}}. \tag{3}$$

Given the target for V_R lies in the range of 0.05–0.2, then Y_{H_2} lies in the range 0.003–0.0125. The relationship between average volume fraction and inlet conditions can be understood from the conservation of mass and species. The conservation of mass requires

$$\frac{1}{4}\pi\rho_1 u_1 d_1^2 + \frac{1}{4}\pi\rho_2 u_2 d_2^2 = \frac{1}{4}\pi\rho_o u_o d_1^2, \tag{4}$$

where the subscript 'o' denotes the output condition. The conservation of hydrogen species requires the injected mass flux of hydrogen to be equal to the flux of homogenous blend leaving 'o', or

$$\frac{1}{4}\pi\rho_2 u_2 d_2^2 = \frac{1}{4}\pi\overline{Y_{H_2,o}}\rho_o u_o d_1^2, \tag{5}$$

where $\overline{Y_{H_2,o}}$ is the average mass fraction of hydrogen at the flow outlet. From (1,2,5,6) the exit mass fraction of the hydrogen is

$$\overline{Y_{H_2,o}} = \frac{M_{H_2}}{M_{CH_4}} \frac{\alpha}{1+\alpha}, \qquad \alpha = \mathcal{D}\frac{p_1}{p_2}\frac{T_2}{T_1}, \tag{6}$$

where the volumetric dilution is

$$\mathcal{D} = \left(\frac{d_2}{d_1}\right)^2 \frac{u_2}{u_1}. \tag{7}$$

This provides a link between the inlet conditions and the exit conditions, expressed in terms of a volumetric dilution factor, pressure and temperature. The inlet pressure differential is small due to the short pipe lengths considered so that $p_1/p_2 \approx 1$. To achieve a target volume fraction, V_R, we look at a sweep over values of volumetric dilution over the range of $\mathcal{D} = 0.05, 0.1, 0.2$ to 0.3, with the geometrical differences of $d_2/d_1 = 1/2, 1/4$. These values define the velocity ratio u_2/u_1 through equation (7). This gives $V_R = 0.047, 0.086, 0.149, 0.196$ respectively. From (1), the ratio of the density of pure hydrogen to pure methane at the inlets is $\frac{\rho_2}{\rho_1} = \frac{M_{H_2}}{M_{CH_4}}\frac{p_1}{p_2}\frac{T_2}{T_1} \sim 1/8$, since $M_{H2}/M_{CH4} = 1/8$ – far larger than the thermal effect since $T_2/T_1 \sim 1.04$. This is an unusually large density contrast for single-phase flows. The momentum ratio of the side branch to the main line,

$$M_R = \frac{\rho_2 u_2^2}{\rho_1 u_1^2} = \frac{M_{H_2}}{M_{CH_4}}\mathcal{D}^2\left(\frac{d_1}{d_2}\right)^4, \tag{8}$$

provides an objective measure of the potential for mixing to occur due to injection. For $M_R < 1$, jet penetration is expected to be weak and this is likely to occur at low dilution factors and larger diameter side branches ($d_2/d_1 = 1/2$).

Mathematical model

Model choice

The physical problem consists of two non-reacting gases mixing as they move through a pipe; the high Reynolds number means that turbulence is a critical feature of the flow. Denoting the velocity as u_i, the pressure p and effective dynamic viscosity μ_e, the conservation of momentum is

$$\frac{\partial(\overline{\rho}u_i)}{\partial t} + \frac{\partial(\overline{\rho}u_i u_j)}{\partial x_j} = -\frac{\partial p}{\partial x_i} + \frac{\partial}{\partial x_j}\left(\mu_e\left(\frac{\partial u_i}{\partial x_j} + \frac{\partial u_j}{\partial x_i}\right)\right) + \overline{\rho}f_i, \tag{9}$$

where f_i is the gravitational body force acting on the flow. The gas species is represented as a mass fraction $Y_*(= Y_{H_2}, Y_{CH_4})$ and are advected according to

$$\frac{\partial(\overline{\rho}Y_*)}{\partial t} + \nabla\cdot(\overline{\rho}Y_*\boldsymbol{u}) = \nabla\cdot(\mu_e\nabla Y_*) \tag{10}$$

The energy equation is cast in terms of the evolution of enthalpy h, where

$$\frac{\partial(\overline{\rho}h)}{\partial t} + \frac{\partial(\overline{\rho}u_i h)}{\partial x_i} + \frac{\partial(\overline{\rho}K)}{\partial t} + \frac{\partial(\overline{\rho}u_i K)}{\partial x_i} - \frac{\partial p}{\partial t} = \nabla\cdot(\mu_e\nabla h) + R_i \tag{11}$$

where the (specific) kinetic energy is $K = 1/2u_i^2$. The temperature is determined iteratively from h – since the temperature variation is small in this study and we set $c_p = h/T$ as a constant for each species. The heat capacities are set as c_p = 14,320 J kg^{-1} K^{-1} and 2231.5, for hydrogen and methane respectively.

Turbulence modelling

There are a large number of models of turbulence that are suitable for describing the closure of the turbulent stresses with strong thermal effects. A validation exercise was organised by [24] who described a comparative study between many different computational models for T-junction mixing of warm and cold water streams. The top ten studies that compared most successfully to the experiments were based on a large-eddy (LES) formulation, typically with a DDES model to better account for turbulence production near a wall whilst taking advantage of the LES model within the flow interior. Based on the outcome of [24], the Spalart-Allmaras DES model [25,26] was applied in this paper; this model introduces a single equation describing the evolution of the turbulent viscosity.

Boundary conditions

Fig. 1 shows the flow geometry of the flow problem. The flow entering the main pipe and branch were set with a standard power-law fit, typical of a turbulent inlet flow, where the normal velocity $u_r = u_*\left(1 - \left(\frac{2r}{d_*}\right)^2\right)^{\frac{1}{n}}$, where r is the distance from the pipe centre on the inlet faces and $n = 7$. The volume flux is $Q_* = nu_*\pi d_*^2/4(n+1)$.

Please cite this article as: Eames I et al., Injection of gaseous hydrogen into a natural gas pipeline, International Journal of Hydrogen Energy, https://doi.org/10.1016/j.ijhydene.2022.05.300

Implementation and validation

The model was solved using standard modules available with OpenFOAM which is a general computational package for solving PDEs in a highly abstracted manner. The standard solver *rhoReactingBuoyantFoam* was applied, tracking the H_2 and CH_4 species. The turbulence model *SpalartAllmaraDDE* was applied, with both combustion and reactions switched off. The mesh was generated using *snappyHexMesh* with an applied boundary layer mesh, refinement in the vicinity of the side branch, but otherwise of uniform size. The mesh varied from 2.8 to 4.8 M cells. Calculations were run up to $t = 5$ and averaged over the period 4–5 *s*.

A validation exercise was performed to test the numerical simulations. Since the mixing process is dominated by the local geometry of the T-junction, a validation case based on this configuration was chosen. The OECD CFD test case [27] involved a comprehensive experimental study of the liquid flow statistics near a T-junction and comparative summary of the results from a number of codes is reported by Ref. [24]. Here we chose [28], characterised by $Q_1/Q_2 = 1$, $d_1/d_2 = 1$, and compared the mean and rms statistics of the streamwise flow. The turbulent flow was calculated for a gas system with a Froude number that matched the branch flow ($Fr = U_2/\sqrt{|\rho_1 - \rho_2|g/\rho_1}$) from Ref. [28]. Fig. 2 shows the setup and comparison between the near field mean flow and statistics for a mesh of 2 M cells which is typical of the mesh quality throughout the study. The agreement is good. We observed that for meshes smaller than 500 k cells, the turbulence statistics tended to be under predicted. The simulations were also compared with the case of a water system, giving a similar accuracy as indicated in Fig. 2(b).

Numerical results

Influence of injection rate

Fig. 3(a) shows the instantaneous volume fraction V_R of hydrogen in a vertical slice through the flow (for a fixed $d_1/d_2 = 1/4$) and the volumetric dilution factor, $\mathcal{D}$, varying from 0.05 to 0.3. For the lowest volume fraction, the momentum ratio $M_R = 0.08$ is sufficiently low that the inlet flow is immediately deflected by the incident flow and the hydrogen is confined to a thin layer near the upper portion of the pipe. The confinement is maintained by the buoyancy difference between the diluted hydrogen mixture and methane.

For $\mathcal{D} = 0.1$, the interaction between the flow in the main line and branch inlet generates an unsteady flow. The unsteadiness is characterised by a timescale approximately determined by the advective speed u_1 past the side branch of diameter d_2 and with a typical Strouhal number of $St \sim 0.2$, giving a shedding frequency of $f_s = u_1 St/d_2$ which is expected to show a weak dependence on u_2. This is confirmed in Fig. 3(a) where the puffs are separated by about 0.8 m. With increasing branch velocity, the penetration increases and starts to interact with the opposite wall beyond $\mathcal{D} = 0.2$. For $\mathcal{D} = 0.3$, the branch flow flaps between two states - shedding along the upper wall and penetrating to the opposite surface.

Fig. 3(b) shows the hydrogen volume fraction averaged over a period of 1s, $\overline{V}_R$, and confirms the confinement of hydrogen in the upper portion of the pipe for $\mathcal{D} < 0.3$ and the jet confinement to the upper and lower walls for $\mathcal{D} = 0.3$. The maximum hydrogen concentration in the vertical plane $\overline{V}_{Rm}$, as function of distance downstream from the branch inlet, is shown in Fig. 3(c). The maximum value $\overline{V}_{Rm}$ is typically much larger than the target value of V_R. The maximum value decreases rapidly from the inlet but the rate of decrease diminishes rapidly as the relative difference in speed between the flow perturbation caused by the buoyant inlet and the mainline decreases, and shear induced mixing is suppressed.

The volume fraction of hydrogen at the pipe wall surface is shown in Fig. 4 for contrasting dilution factors (at $t = 5$ s). For low dilution factors ($\mathcal{D} < 0.3$), the hydrogen is confined to the upper portion of the pipe and that the pipe is exposed to pure hydrogen a distances greater than $\sim d_1$ downstream of the injection point. When $\mathcal{D} = 0.3$, the hydrogen jet interacts with the opposite wall with the hydrogen concentration higher on the lower inner surface.

The characteristics of the pipe surface hydrogen concentration is shown in Fig. 5 which contrasts the instantaneous (Fig. 5(a)) and average (Fig. 5(b)) wall concentrations. Central to the degree of mixing is the location of the highest hydrogen

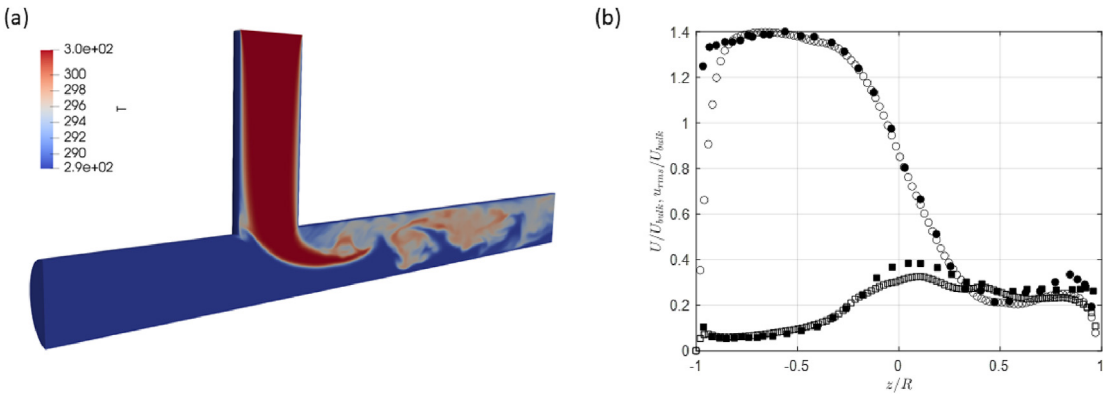

Fig. 2 – (a) Validation exercise using [28] with $Q_1/Q_2 = 1$, $d_1/d_2 = 1$. The geometrical configuration is shown along with the *T* distribution at $t = 10$. The main channel flow is $T_1 = 2888$ K with $T_2 = 303$K. (b) Mean and rms streamwise velocity in the centreline vertical plane a distance $1.86d_1$ from the branch inlet, compared with the experimental measurements.

Please cite this article as: Eames I et al., Injection of gaseous hydrogen into a natural gas pipeline, International Journal of Hydrogen Energy, https://doi.org/10.1016/j.ijhydene.2022.05.300

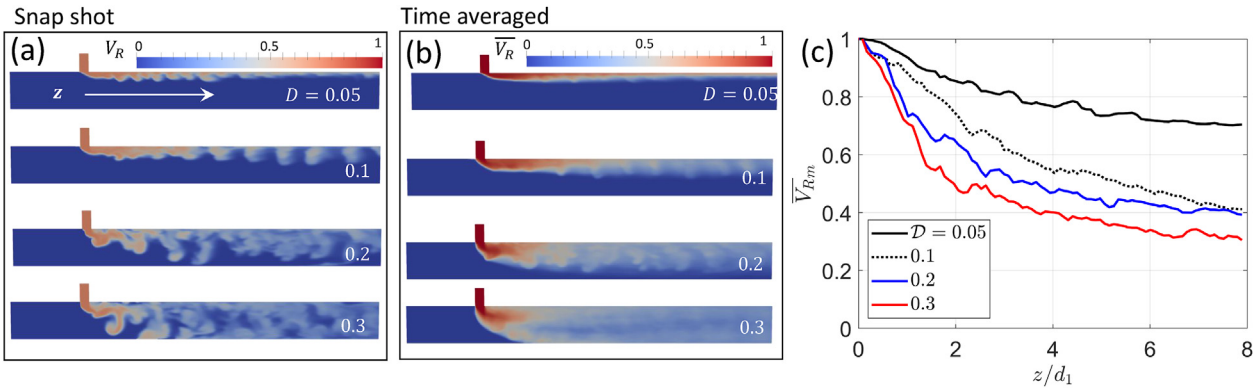

Fig. 3 – The sequence indicates the influence of dilution factor on the distribution of hydrogen in the flow interior. In (a), the instantaneous dstribution of hydrogen volume fraction V_R is shown and contrasts with the time averaged distribution $\overline{V}_{Rm}$ in (b). The maximum of $\overline{V}_R$ as a function of distance z from the branch inlet is plotted for different dilution factors in (c).

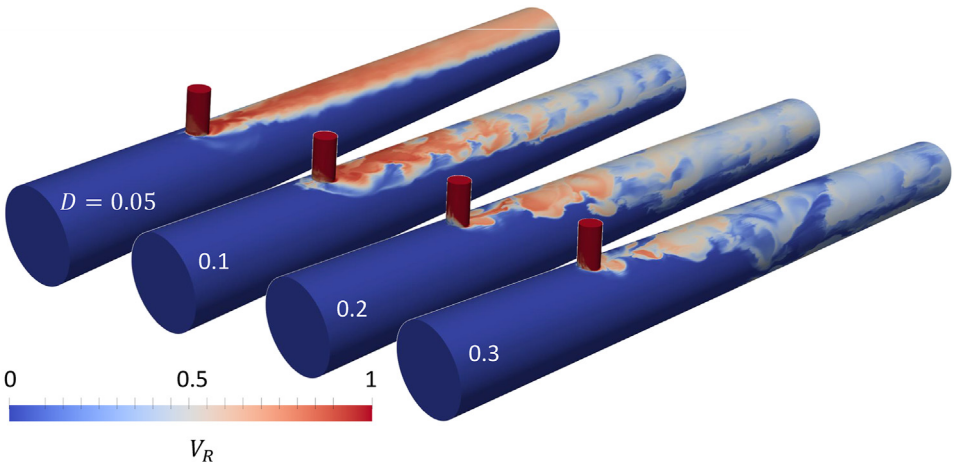

Fig. 4 – Inclined view of flow hydrogen injected into a methane main line for dilution factors $\mathcal{D} = 0.0$, 0.1, 0.2 and 0.3. The molar fraction or volume fraction V_R of hydrogen on the pipe wall is plotted as a colour map. The pipe ratio diameters are $d_2/d_1 = 1/4$. (For interpretation of the references to colour in this figure legend, the reader is referred to the Web version of this article.)

concentration - whether it occurs on the surface of the pipe or the flow interior. Fig. 5(c) shows a comparison between the interior and wall bounded maximum concentrations obtained from Figs. 3(b) and 4(b). The maximum hydrogen concentration occurs within the flow interior near the injection point with the oscillatory movement of the side jet (as evident in Fig. 4) leading to a reduction of the average concentration rather than due to dilution through entrainment. Beyond approximately $\sim 2d_1$ downstream of the branch, the maximum of the average hydrogen concentration occurs at the wall mainly as a consequence of buoyancy effects. The average hydrogen concentration on the wall provides a measure of the exposure of pipe material to hydrogen.

Influence of branch pipe diameter

The influence of a larger diameter pipe branch is shown in Fig. 6(a,i). The immediate consequence is clear – increasing the pipe diameter decreases the exit velocity and since the momentum flux M_R has a strong dependence on velocity, the penetrative distance is greatly reduced. Although the exit velocity u_2 increases by a factor of 6 (from $\mathcal{D} = 0.05$ to 0.3), the shedding frequency in Fig. 6(a,i) has a relatively weak dependence on $\mathcal{D}$. The snap shots give an appearance of a steady near field, however, they have captured the shedding process at a similar stage in the cycle. The coherent vortices shed into the pipe flow interior, that contain a high concentration of hydrogen, are quickly accelerated to the mean ambient flow. Further downstream, the relative speed between the vortices, that contain hydrogen, and the ambient flow, decreases and the buoyant regions have a stronger tendency to rise in the pipe.

Influence of pipe orientation

Fig. 6(b) show the influence of Hillside injection. Since the injected flow slows more rapidly as it interacts more strongly with the side wall, the concentration of hydrogen on the wall

Please cite this article as: Eames I et al., Injection of gaseous hydrogen into a natural gas pipeline, International Journal of Hydrogen Energy, https://doi.org/10.1016/j.ijhydene.2022.05.300

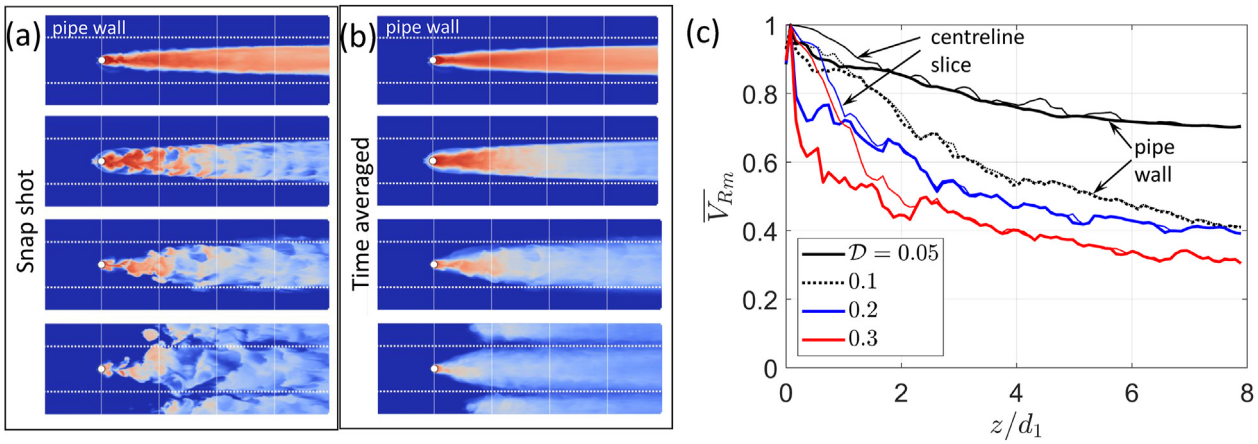

Fig. 5 – (a) Variation of the maximum volume fraction of hydrogen V_R (on the wall of the mainline) with distance from the branch inlet. The curves denote the (b) The instantaneous volume fraction of hydrogen on the surface of the pipe is shown for volumetric dilution factor $\mathcal{D} = 0.05$, 0.1, 0.2 and 0.3. The surface of the pipe is unwrapped. The separation of the vertical lines show the distance $2d_1$.

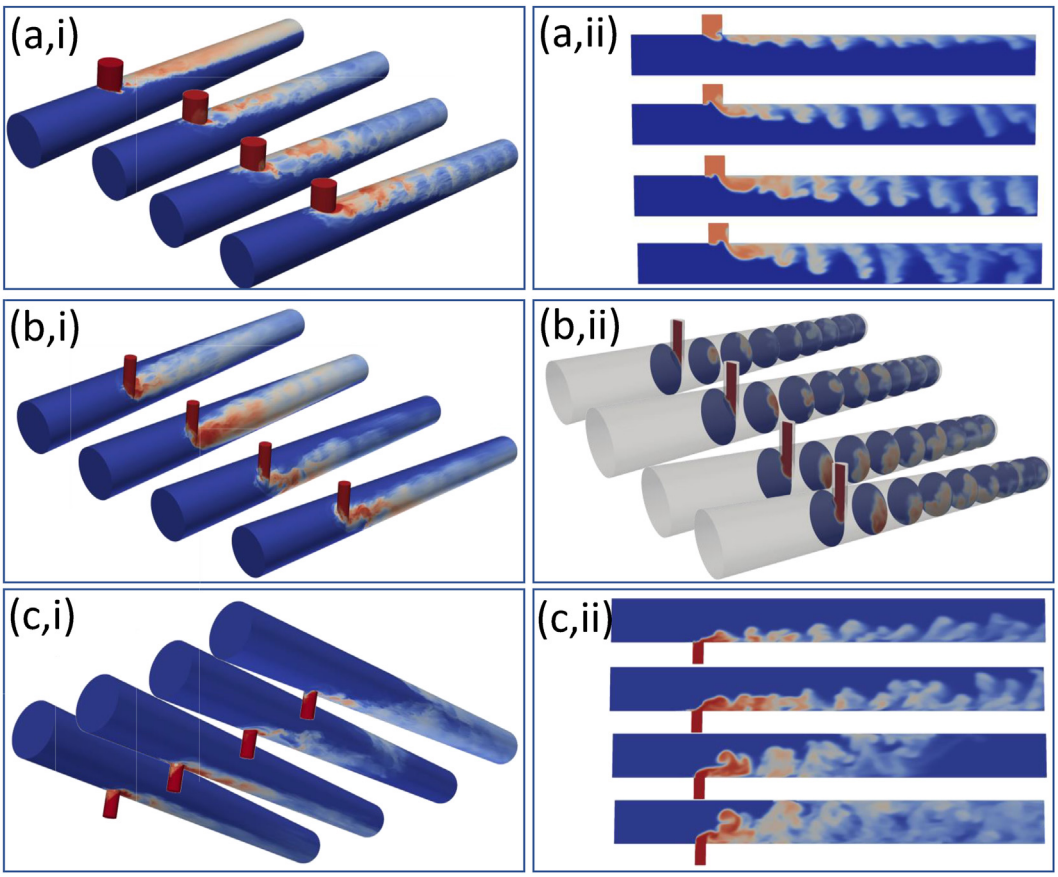

Fig. 6 – Summary of the influence of changing the branch geometry on the surface and interior concentration of hydrogen. In (a) the effects of a larger branch top-side inlet ($d_2/d_1 = 1/2$), (b) a Hillside inlet ($d_2/d_1 = 1/2$) and (c) bottom-side inlet are shown.

is larger than in the case of direct vertical injection. The effectiveness of mixing by Hillside injection is reduced by the jet buoyancy and wall drag both acting in opposite direction to the momentum flux of the inlet jet.

Fig. 6(c) shows the influence of bottom-side injection on mixing. Buoyancy forces and momentum flux are orientated in the same direction, leading to the hydrogen mixture rise to the top surface of the pipe and a reduction of the hydrogen

Please cite this article as: Eames I et al., Injection of gaseous hydrogen into a natural gas pipeline, International Journal of Hydrogen Energy, https://doi.org/10.1016/j.ijhydene.2022.05.300

concentration on the lower wall. The rise of the mixed hydrogen through the methane enhances mixing compared to top-side injection. At the lowest $\mathcal{D}$, the hydrogen layer rises through the layer of methane towards the top surface, while for higher dilution factors and faster injection speed leads to a pure hydrogen impinging on the top pipe wall.

Fig. 7(a) shows how the average maximum wall concentration varies for bottom-side injection and different dilution factors. In the near field, the hydrogen for the lowest dilution rate ($\mathcal{D} = 0.05$), rises leading to a rapid reduction on the lower wall. For $\mathcal{D} = 0.1$, the near jet penetration distance is limited by the incident flow, pushing the hydrogen along the wall, causing it to interact with the lower wall and a higher concentration than for lower, and higher, dilution factors. For $\mathcal{D} > 0.1$, the unsteady shedding and subsequent rise, leads to mixing and lower concentrations on the pipe wall. To understand how these values relate to the target hydrogen concentration, the ratio of the hydrogen concentration to the target value ($V_{R,T}$) are plotted in Fig. 7(b); a value of $\mathcal{R} = \overline{V}_{Rm}/V_{R,T} = 1$ provides a measure of mixing. Fig. 7(b), shows that at 8 pipe diameters from the injection point, the maximum hydrogen concentration at the wall varies from 4.4 to 1.6 times the target hydrogen volume concentration, as the target varies from 5% to 20%.

Implications for hydrogen injection into pipes

Near field

The well-documented occurrence of hydrogen embrittlement in steels and the modelling results presented here, clearly indicate that there will be an increased susceptibility to component failure in and around hydrogen injection points. The susceptibility to hydrogen embrittlement is a function of hydrogen concentration and our model has revealed hydrogen concentrations that far exceed the average dilution factors (Fig. 6). The fact that high concentrations have been shown to occur close to the inner surface of pipeline material is of further concern as is the knowledge that the codes extending the use of pipes to mixed gas delivery may not explicitly recognise the inhomogeneities that we have seen. There are two challenges which must be addressed separately:

(a) Side branch pipe - the presence of high pressure pure hydrogen means that material selection is critical here. This could be achieved using steel pipe with a thicker wall thickness or switching to fiberglass pipe system designs or lined steel pipes.
(b) Header pipe - the results highlight the need to mix the hydrogen near the injection point. The sweep over different injection configurations suggests that simple changes to the inlet point are not sufficient to accomplish uniform mixing. This could be accomplished with a passive inline mixers, such as a porous plate.

Design selection and implications

The choice of pipe dimensions are specified in design codes, for example ASME B31.3 (Pressure Design of Piping Components) [10], which places constraints on wall thickness and internal pressure when hydrogen is present. This reflects the fact that crack growth rates increase by a factor of 10^4 at low levels of hydrogen ($<5\%$) but become less sensitive at higher concentrations. Hydrogen interacts with the internal structure of steels via a diffusive process which is extremely slow typically $D_{H_2} \sim 10^{-11} m^2/s$. The long timescale for hydrogen interaction with steel pipes (with thickness ΔR) is set by a diffusive time $t \sim \Delta R^2/D_{H_2} \sim (10^{-2}\ \mathrm{m})^2/(10^{-11}\ \mathrm{m}^2\ \mathrm{s}^{-1}) = 10^7 \mathrm{s}$, or 4 months, highlighting that the consequence of material changes due to hydrogen embrittlement, will occur over years.

Traditionally the pressure (p_i, without hydrogen), mass flux and material selection constraints dictate pipe diameter (d_2) and wall thickness (ΔR). Here the inverse question remains for a piping network that is to be repurposed to carry hydrogen - given the pipe diameter, material selection and wall thickness, what constraints are placed on the system, specifically the gas pressure with hydrogen p_h. A traditional design selection defines a minimum pipe wall thickness

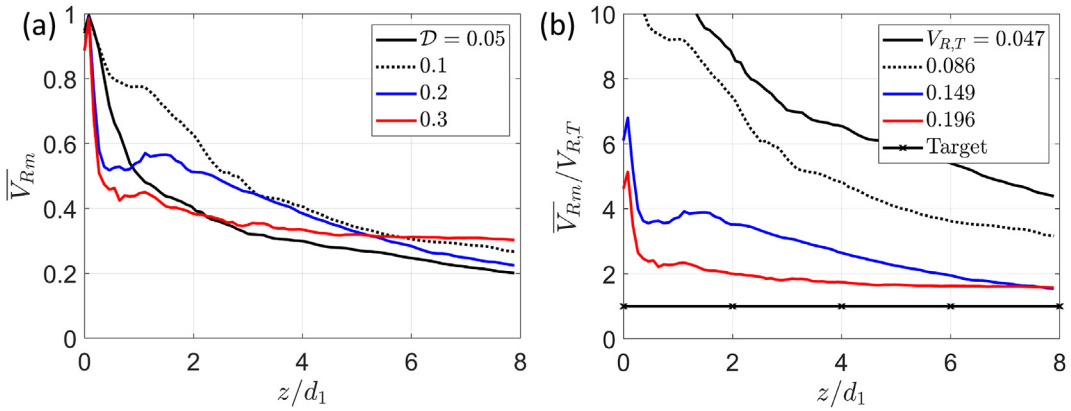

Fig. 7 – (a) The variation of average maximum hydrogen concentration on the pipe wall ($\overline{V}_{Rm}$) for the bottom-side injection. (b) Ratio of the average maximum wall concentration to target value $V_{R,T}$, as a function of downstream distance from the side branch. The horizontal dashed line is perfect mixing.

Please cite this article as: Eames I et al., Injection of gaseous hydrogen into a natural gas pipeline, International Journal of Hydrogen Energy, https://doi.org/10.1016/j.ijhydene.2022.05.300

Table 1 – Mandatory factor M_f for carbon steel pipes at pressures less than 6.9 MPa (or 1000 psi). Taken from Tables IX–5B Carbon Steel Piping Materials Performance, p. 215 [10].

Range of Tensile strength (ksi)	≤ 70	(70, 75]	(75, 80]	(80, 90]
Yields stress (ksi)	≤ 52	≤ 56	≤ 65	≤ 80
M_f	1.0	0.930	0.839	0.715

$$\Delta R + c, \tag{12}$$

where ΔR is determined from

$$\Delta R = \frac{p_i d_1}{2(SEM_f + p_1 Y)}, \tag{13}$$

(when $\Delta R < d_2/6$), p_i is the internal gage pressure, and S (Tables IX–1A) is the stress value for the pipe material, and an offset c that is comprised of a sum of mechanical allowances for corrosion and erosion. The minimum wall thickness (or the nearest thickness) is usually chosen due to cost constraints. The factors E (Tables IX–2 or Tables IX–3A, p. 204), M_f (see Table 1) and Y are measures that depend on quality factor (mandatory Appendix IX, p.180). M_f addresses the loss of material ductility in hydrogen services (Tables IX–5B Carbon Steel Piping Materials Performance, p. 215). Since the pipe wall thickness is currently fixed, the maximum internal pressure that can be set in the presence of hydrogen becomes

$$p_h = \frac{2SEM_f \Delta R}{p_1 - \Delta R}. \tag{14}$$

or

$$p_h = p_i M_f. \tag{15}$$

This means that pipe designs close to the minimum thickness envelope (13) would require a reduction in the operating pressure by a factor of M_f (see Table 1). This needs to be taken into account for steels with yields stress greater than 52 ksi.

Conclusion

We have explored the implications of hydrogen injection via a T-junction into a natural gas pipe using a computational model. The relationship between the target blend volume fraction V_R and local parameters are described by (2, 3) and (6), which shows that the blend ratio is primarily determined, but not wholly, by the volumetric dilution effect.

The low molecular mass of hydrogen has two important effects on the injection process: (a) the inertia of the injected gas stream is low so that penetration is limited, and (b) the hydrogen is buoyant and tends to be stratified. Both effects lead to higher hydrogen concentration near the top section of the pipe. An analysis of the different pipe injection configurations indicates that mixing is greatest when injected from the bottom so that hydrogen has the potential to rise through the pipe flow. The maldistribution of hydrogen has implications for concentrated embrittlement of the pipe wall. It has been noted that embrittlement is significant near welds. To promote mixing, it is recommended to use a passive inflow mixer.

The computational model provides a leading order description of these process which are dominated by the injection process and buoyancy effects. The inlet conditions are set as uniform inlet profiles which neglect the effect of turbulence generated by the pipe walls or upstream infrastructure (such as valves or bends). These additional processes will enhance mixing process and so the model provides an indication of the worst case scenario.

An analysis of ASME code of practice indicates that X52 carbon steel could be operated with hydrogen blends. High tensile steels, being more susceptible to embrittlement, require a reduction of static line pressure, by 7% for X56 and 16% for X65. In contrast, the competing demand to maintain a constant energy density (per unit volume) following the introduction of hydrogen, will likely require an increase in static pressure [9]. The contrasting demands of the pipe network safety and the user energy demands will certainly need to be addressed in the future.

Our analysis has shown that the injection of pure gaseous hydrogen into a methane pipeline leads to hydrogen concentrations on wall near the injection branch much higher than the average concentration. The low hydrogen density means that buoyancy plays an important role in maintaining hydrogen stratified downstream of the injection points. Both factors mean that the poor mixing of hydrogen following its injection into methane or natural gas can significantly raise the risk of component failure and pipeline rupture. To ensure that the energy flux of a hydrogen blend delivered to customers is maintained, either the gas flow rate or pressure must be increased, which increases the risk of fatigue due to acoustic-induced vibration. Our future work is centered around assessing this compound risks.

Credit author statement

Ian Eames: Conceptualisation, modelling and data analysis.

Mike Austin: Industrial context and design codes.

Adam Wojcik: Discussion of hydrogen on materials, drafting.

Declaration of competing interest

The authors declare that they have no known competing financial interests or personal relationships that could have appeared to influence the work reported in this paper.

Acknowledgements

The authors acknowledge the use of UCL High-Performance Computing Facilities (Kathleen@UCL) and their unparalleled support services.

REFERENCES

[1] Guandalini G, Colbertaldo P, Campanari S. Dynamic modeling of natural gas quality within transport pipelines in presence of hydrogen injections. Appl Energy 2017;185:1712–23. https://doi.org/10.1016/j.apenergy.2016.03.006. clean, Efficient and Affordable Energy for a Sustainable Future, https://www.sciencedirect.com/science/article/pii/S0306261916303178.

[2] Schouten J, Janssen-van Rosmalen R, Michels J. Modeling hydrogen production for injection into the natural gas grid: balance between production, demand and storage. Int J Hydrogen Energy 2006;31(12):1698–706. https://doi.org/10.1016/j.ijhydene.2006.01.005. https://www.sciencedirect.com/science/article/pii/S0360319906000243.

[3] Wahl J, Kallo J. Quantitative valuation of hydrogen blending in european gas grids and its impact on the combustion process of large-bore gas engines. Int J Hydrogen Energy 2020;45(56):32534–46. https://doi.org/10.1016/j.ijhydene.2020.08.184.

[4] Cheli L, Guzzo G, Adolfo D, Carcasci C. Steady-state analysis of a natural gas distribution network with hydrogen injection to absorb excess renewable electricity. Int J Hydrogen Energy 2021;46(50):25562–77. https://doi.org/10.1016/j.ijhydene.2021.05.100.

[5] Elaoud S, Hafsi Z, Hadj-Taieb L. Numerical modelling of hydrogen-natural gas mixtures flows in looped networks. J Petrol Sci Eng 2017;159:532–41. https://doi.org/10.1016/j.petrol.2017.09.063.

[6] Melaina MW, Antonia O, Penev M. Blending hydrogen into natural gas pipeline networks: a review of key issues. National Renewable Energy Laboratory; 2013. Prepared under Task No. HT12.2010.

[7] Dodds PE, McDowall W. The future of the UK gas network. Energy Pol 2013;60:305–16. https://doi.org/10.1016/j.enpol.2013.05.030.

[8] [link].URL https://www.iea.org/data-and-statistics/charts/limits-on-hydrogen-blending-in-natural-gas-networks-2018.

[9] Liu J, Teng L, Liu B, Han P, Li W. Analysis of hydrogen gas injection at various compositions in an existing natural gas pipeline. Front Energy Res 2021;9:368.

[10] ASME. Hydrogen piping and pipelines ASME code for pressure piping, B31. ASME; 2012.

[11] Kok J, van der Wal S. Mixing in t-junctions. Appl Math Model 1996;20:232–43.

[12] Turner JS. Buoyancy effects in fluids, cambridge monographs on mechanics. Cambridge University Press; 1973. https://doi.org/10.1017/CBO9780511608827.

[13] Hamzehloo A, Aleiferis PG. Large eddy simulation of highly turbulent under-expanded hydrogen and methane jets for gaseous-fuelled internal combustion engines. Int J Hydrogen Energy 2014;39(36):21275–96.

[14] Crunteanu D, Isac R. Investigation of low emission combustors using hydrogen lean direct injection. INCAS BULLETIN 09 2011;3. https://doi.org/10.13111/2066-8201.2011.3.3.5.

[15] Kickhofel J, Prasser H-M, Selvam PK, Laurien E, Kulenovic R. T-junction cross-flow mixing with thermally driven density stratification. Nucl Eng Des 2016;309:23–39. https://doi.org/10.1016/j.nucengdes.2016.08.039.

[16] CFD modeling of thermal mixing in a T-junction geometry using les model. Nucl Eng Des 2012;253:183–91. https://doi.org/10.1016/j.nucengdes.2012.08.010. sI : CFD4NRS-3.

[17] Evrim C, Chu X, Laurien E. Analysis of thermal mixing characteristics in different t-junction configurations. Int J Heat Mass Tran 2020;158:120019.

[18] Miyoshi K, Kamaya M, Utanohara Y, Nakamura A. An investigation of thermal stress characteristics by wall temperature measurements at a mixing tee. Nucl Eng Des 2016;298(C):109–20. https://doi.org/10.1016/j.nucengdes.2015.12.004.

[19] Kamaya M, Miyoshi K. Thermal fatigue damage assessment at mixing tees (elastic-plastic deformation effect on stress and strain fluctuations). Nucl Eng Des 2017;318:202–12. https://doi.org/10.1016/j.nucengdes.2017.04.022.

[20] Timperi A. Development of a spectrum method for modelling fatigue due to thermal mixing. Nucl Eng Des 2018;331:136–46. https://doi.org/10.1016/j.nucengdes.2018.02.039.

[21] Hirth JP. Effects of hydrogen on the properties of iron and steel. Metall Trans A 1980;11(6):861–90. https://doi.org/10.1007/BF02654700.

[22] Slifka A, Drexler E, Amaro R, Hayden L, Lauria D, Hrabe N, Stalheim D. Fatigue measurement of pipeline steels for application of gaseous hydrogen transport. 2018. https://doi.org/10.1115/1.4038594.

[23] Bains M, Hill L, Rossington P. Environmental Agency. 2018. https://assets.publishing.service.gov.uk/government/uploads/system/uploads/attachment_data/file/545567/Material_comparators_for_fuels_-_natural_gas.pdf.

[24] Smith B, Mahaffy J, Angele K. A CFD benchmarking exercise based on flow mixing in a t-junction. Nucl Eng Des 2013;264:80–8. https://doi.org/10.1016/j.nucengdes.2013.02.030. sI:NURETH-14, https://www.sciencedirect.com/science/article/pii/S0029549313000897.

[25] Spalart P, Allmaras S. A one-equation turbulence model for aerodynamic flows. Recherche Aerospatiale 1994;1:5–21.

[26] Spalart MSPR, Jou W-H, Allmaras S. Comments on the feasibility of LES for wings, and on a hybrid RANS/LES. Advances in DNS/LES 1997:137–47.

[27] Höhne T. Scale resolved simulations of the OECD/NEA–vattenfall T-junction benchmark. Nucl Eng Des 2014;269:149–54. https://doi.org/10.1016/j.nucengdes.2013.08.021.

[28] Braillard O, Howard R, Angele K, Shams A, Edh N. Thermal mixing in a T-junction: novel CFD-grade measurements of the fluctuating temperature in the solid wall. Nucl Eng Des 2018;330:377–90. https://doi.org/10.1016/j.nucengdes.2018.02.020.

Please cite this article as: Eames I et al., Injection of gaseous hydrogen into a natural gas pipeline, International Journal of Hydrogen Energy, https://doi.org/10.1016/j.ijhydene.2022.05.300